Mode Coupling Theory and the Glass Transition in Molecular Dynamics Simulated NiZr

H. Teichler

Institut fur Metallphysik, University of Göttingen and Sonderforschungsbereich 345, D-37073 Göttingen, Germany

(Received 23 February 1995)

Molecular dynamics (MD) simulations for a NiZr model adapted to Hausleitner-Hafner interatomic potentials are analyzed within the mode coupling theory (MCT). Fitting numerical solutions of the (modified) schematic MCT equation with the self-intermediate scattering function of the MD system demonstrates unambiguously the transition scenario from liquidlike to nearly arrested behavior predicted by the MCT as precursor of the glass transition (around 1120 K for the present NiZr model).

PACS numbers: 61.20.Ja, 64.70.Pf

The liquid-glass transition [1,2] is one of the unsolved challenging problems in present solid state theory. In contrast to usual phase transformations the glass transition (GT) seems to be primarily dynamic in origin. Therefore new theoretical approaches have to be developed for its description. Our Letter is concerned with the self-trapping transition predicted by the mode coupling theory (MCT) [2–8] for undercooled liquids as precursor of the GT at a critical T_c above the glass temperature T_G. At T_c the system is expected [6–8] to approach from higher temperatures the border between the liquidlike "ergodic" and a solidlike arrested "nonergodic" behavior without, however, crossing the boundary but remaining on the ergodic side in a "nearly arrested" state. States beyond the border are not accessible since the strictly arrested self-trapped state ascribed to this regime is an oversimplification that neglects any diffusion and transverse currents in the solid [6–8].

This scenario has not yet been clearly identified so far, neither from experiments nor from computer simulations. Experiments, from the early neutron scattering and spin echo measurements [9] up to the recent light scattering [10] and Raman scattering [11] studies, and molecular dynamics (MD) simulations (e.g., [12–17]) greatly succeeded to reconfirm particular features of the MCT, like the α and β regimes in the decay of density fluctuations in the undercooled liquid. (An extensive compilation of experimental and MD studies is provided, e.g., by [16], including T_c estimations.) The quantitative comparison of MCT results with experiments and MD data concerns so far the scaling properties of the asymptotic law for the α decay [8–17] or of the frequency dependence of the dynamical susceptibilities [9,11–16] in the α and β regimes. But here the work of van Megen and Underwood [10] needs to be mentioned which analyzes light scattering data at colloidal suspensions in terms of solutions of the full MCT for the α regime. Regarding the early β regime, studies (e.g., [11–16]) revealed discrepancies between the observations and MCT which in [11] are ascribed to vibrational atomic motions not fully taken into account in the MCT.

We demonstrate here that MD simulations for a $Ni_{0.5}Zr_{0.5}$ adapted model of a binary transition metal glass are able to verify the T_c transition scenario, that is, the so-called schematic MCT equation with suitable modifications reproduces (quantitatively) the dynamics of the system as obtained from MD modeling, making unambiguously visible the T_c scenario.

Our MD simulations are carried out as state-of-the-art isothermal-isobaric (N, T, p) calculations. The Newtonian equations of $N = 648$ atoms are numerically integrated by a fifth order predictor-corrector algorithm (time step $\Delta t = 2.5 \times 10^{-15}$ s) in a cubic volume with periodic boundary conditions and variable box length L. With regard to the electron theoretical description of the interatomic potentials in transition metal alloys by Hausleitner and Hafner [18] we model the interatomic couplings as in [17] by a volume dependent electron-gas term $E_{\mathrm{vol}}(V)$ and pair potentials $\phi(r)$ adapted to the equilibrium distance, depth, width, and zero of the Hausleitner-Hafner potentials [18] for $Ni_{0.5}Zr_{0.5}$. For this model quasistationary structures are generated by "cooling" the system from 3000 K with cooling rate $-\partial T = 2.5 \times 10^{12}$ K/s and afterwards relaxing the configurations during additional 10^6 integration steps. The time evolution of these configurations then is studied over up to 10^6 integration steps.

The central object of our analysis is the self-part of the intermediate scattering function

$$\Phi(q, \tau) = \langle\langle \exp\{i\mathbf{q} \cdot [\mathbf{x}_j(t_\nu + \tau) - \mathbf{x}_j(t_\nu)]\}\rangle\rangle \qquad (1)$$

(double brackets denote averages regarding atoms j and time points t_ν). Figure 1(a) presents the results evaluated from our MD data in a time window between 15 fs and about 1 ns for wave vector $q = 2\pi(n/L, 0, 0)$ with $n = 8$ (which corresponds to $|q| = 21.6\ \mathrm{nm}^{-1}$), Fig. 1(b) for $n = 4$ ($|q| = 10.8\ \mathrm{nm}^{-1}$). Figures 1(a) and 1(b) display the average over the star of the six q vectors which are equivalent on assuming equivalence of the simulation cube axis and their inverses. The close resemblance of the present data with the experiments (e.g., [10]) and the previous MD studies (e.g., [12–17]) should be stressed here.

 0031-9007/96/76(1)/62(4)$06.00

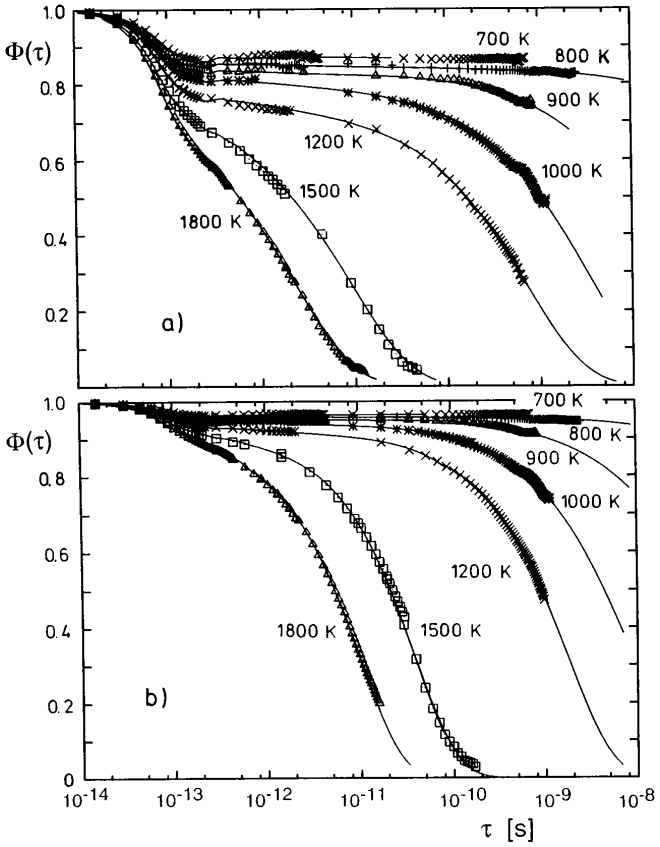

FIG. 1. Self-intermediate scattering functions $\Phi(\tau)$ from MD simulations (symbols) and adapted numerical solutions of the schematic MCT equation for (a) wave vector $q = 21.6\ \mathrm{nm}^{-1}$ and (b) $q = 10.8\ \mathrm{nm}^{-1}$.

To analyze quantitatively the results, we start with the schematic one-component version of the MCT [2], which models the time dependence of structural correlation functions $\Phi(\tau)$ by solutions of

$$\partial_\tau^2\Phi + \eta\partial_\tau\Phi + \omega^2\Phi + \omega^2\int_0^\tau d\tau' f(\tau - \tau')\,\partial_\tau\Phi(\tau') = 0 \qquad (2)$$

[initial conditions $\Phi(0) = 1$, $\partial_\tau\Phi(0) = 0$] with the time dependence of the retarded dissipation kernel governed by the time dependence of $\Phi(\tau)$ itself, i.e., $f(\tau) = f(\Phi(\tau))$.

In our analysis we investigate whether there exist suitable quantities ω, η, and $f(\Phi)$ that bring the numerical solutions of Eq. (2) into agreement with the MD data. ω is fixed by the short-time behavior of $\Phi(q,\tau)$. For this regime Eq. (1) gives $\Phi(q,\tau) = \exp\{-q^2\langle 1/M\rangle kT\tau^2/2\}$, with $\langle 1/M\rangle = (1/M_{\mathrm{Ni}} + 1/M_{\mathrm{Zr}})/2$. This agrees well with the numerical results in Fig. 1 and leads to

$$\omega^2 = q^2\langle 1/M\rangle kT\,.$$

The dissipative kernel $f(\Phi)$ enters the height of the plateau regime of $\Phi(q,\tau)$ at intermediate times as well as the relaxation time of the final α decay and the slope there. From tests it turned out that solutions of (2) using the rather common four-parameter approach $f(\Phi) = F_{p,r} := \lambda_p\Phi^p + \lambda_r\Phi^r$ with p and r independent of T failed to reproduce the MD data. In particular, fitting the data for the two different q values requires different pairs (p,r). To overcome this and to incorporate it in our treatment in a simple manner we used the two-parameter "multiboson" form

$$f(\Phi) = \gamma[\exp(\mu\Phi) - P], \qquad P = 1\,, \qquad (3)$$

taking advantage of the fact that the MCT analysis of the T_c scenario basically relies on a monotonic increase of $f(\Phi)$ with Φ. The form (3) for $f(\Phi)$ is in agreement with the results of the full MCT [3] where sums of pairs of correlators with different q enter the dissipative kernel f. Accordingly, the structure of $f(\Phi)$ reflects nonlinearities in the relationship between the considered $\Phi(q)$ and the correlators with different q' in the kernel. $f(\Phi)$ in the form (3) provides (with P a suitable polynomial in $\mu\Phi$) similar bifurcation singularities and decay laws like an $F_{p,r}$ model. The bifurcation scenario of the form (3) corresponds to that of the $F_{1,2}$ model [5]: For $\mu > 2$ the bifurcation is characterized through an A_2 Whitney fold and type B transitions; for $\mu = 2$ an A_3 cusp with nonergodicity parameter $\Phi_0^c = 0$ gives the end point of the type B transition line, while $\mu < 2$ yields type A transitions. [Setting $P = 1 + (\mu\Phi)^2/2$ gives the bifurcation scenario of the $F_{1,3}$ model [4,5] with an A_3 cuspoidal end point at $\Phi_0^c = 0.4549$ for $\mu = \mu_c = 3.1676$ and elsewhere a Whitney fold, where type A transitions are found for $\mu < \mu_c$.] As within the $F_{p,r}$ models the exponential parameter λ, which determines the decay properties around T_c, is given by $\lambda = (1 - \Phi_0^c)^3\partial^2\Phi^f(\Phi_0^c)/2$.

From the MCT (e.g., [2,3]) it follows that

$$g(\Phi) = f(\Phi)\,(1/\Phi - 1) \qquad (4)$$

(with $\Phi \in [0,1]$) is the relevant quantity that governs the behavior of $\Phi(\tau)$: If for a given T solutions $g(\Phi_k) = 1$ exist then structural arrest occurs [i.e., $\Phi(\tau \to \infty) = \Phi_0 := \mathrm{Max}\{\Phi_k\}$] while in the other case correlations among the fluctuations decay to zero with time. The form (3) for $f(\Phi)$ yields for $g(\Phi)$ a maximum at $\Phi_m \in [0,1]$. In the following we use $g_m := g(\Phi_m)$. The value of g_m reflects whether the system is able to undergo a structural arrest ($g_m > 1$) or whether it remains in the (undercooled) liquid state ($g_m < 1$). In our analysis we consider Φ_m, g_m as independent parameters which are selected to reproduce the MD data by numerical solutions of Eq. (2), exploiting the fact that for the type B transitions there is a one-to-one correspondence between (γ,μ) in (3) and (Φ_m, g_m).

Equation (2) with the modifications discussed so far cannot account for the structure of $\Phi(q,\tau)$ around $\tau = 3\times 10^{-13}$ s, i.e., in the late phonon and early β regime, as demonstrated by Fig. 2. There we display by broken

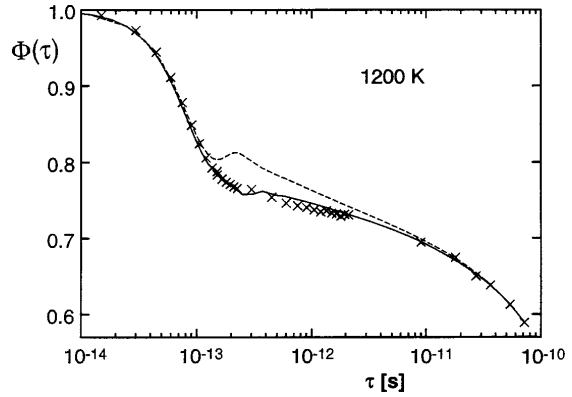

FIG. 2. Part of the 1200 K MD data for $\Phi(\tau)$ at $q = 21.6\ \mathrm{nm}^{-1}$ and fit solutions of Eq. (2) with constant damping term (dashed line) and the retarded damping of Eqs. (5) and (6) (solid line).

lines for the 1200 K data a best-fit solution of (2) with constant damping η which is constructed by demanding to fit well the MD data in the short- and long-time regimes. It fails, apparently, in the early β regime where the MCT predicts the critical power law $\Phi(\tau) = \Phi_0^c + B/\tau^a$. (Similar deviations are found at all temperatures considered.) Comparable deviations from the MCT predictions for this regime are known from analyzing the frequency dependence of the dynamical susceptibility of MD data [12–16] and, recently, of Raman scattering results [11]. In the latter study these deviations are attributed to vibrational atomic motions not fully taken into account in the MCT. (Also relations to the "boson peak" are considered there.) To model this structure with sufficient accuracy, we substitute the instantaneous damping term into (2) by a retarded expression

$$\eta\,\partial\Phi \rightarrow \int_0^\tau d\tau' h(\tau - \tau')\partial_\tau \Phi(\tau')\,, \tag{5}$$

$$h(\tau) = a\,\mathrm{Re}\{\exp(-b\tau + i\Omega\tau + i\psi)\}\,. \tag{6}$$

An acceptable fit of the numerical data for the considered temperatures and q values is achieved with $a = 3.85 \times 10^{23} T/\mathrm{K\,s}^2$, $b = 1.19 \times 10^{10} T/\mathrm{K\,s}$, $\Omega = 2\pi/(3 \times 10^{-13}\ \mathrm{s})$, $\psi = 0.4\pi\omega(10^{-10}/T)\ \mathrm{K\,s}$. The full lines in Fig. 2 display the fit obtained with these parameters.

The results of our analysis are included in Figs. 1(a) and 1(b) by solid lines. They present numerical solutions of (2) with parameters g_m and Φ_m selected via trial and error to fit the MD data. Figures 3(a) and 3(b) display the corresponding values of g_m and Φ_m. For $T > 700$ K the trial-and-error procedure fixes the parameters well. At 700 K and below no α-type decay is seen in the time window accessible to our MD simulations. This limits the independent determination of both parameters below this temperature. Thus for 700 and 600 K, Φ_m is extrapolated from higher T values. g_m is determined throughout from the MD data where fitting the curves

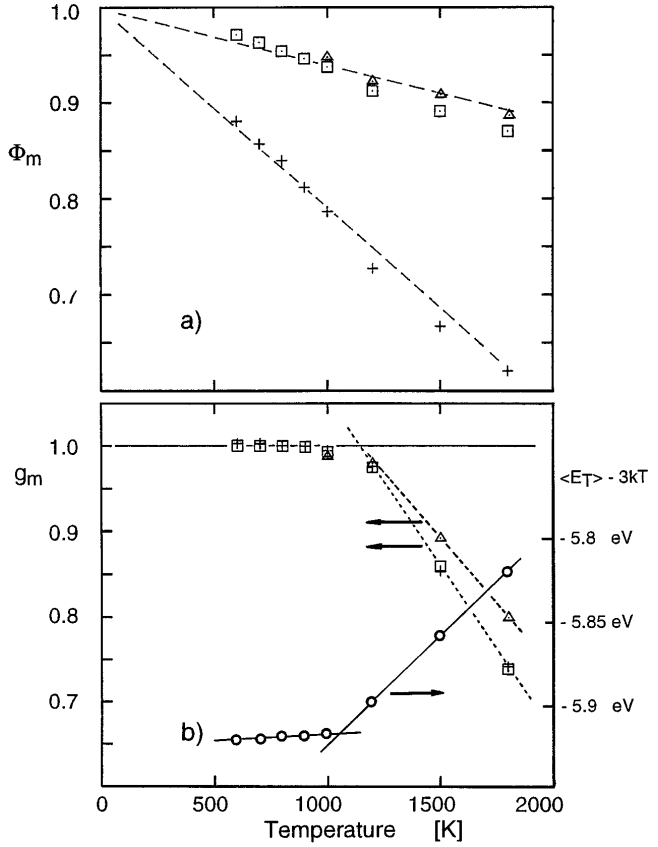

FIG. 3. Parameters Φ_m, g_m (left-hand scale) obtained by adapting solutions of the MCT equation to the MD self-intermediate scattering function (crosses $q = 21.6\ \mathrm{nm}^{-1}$, squares $q = 10.8\ \mathrm{nm}^{-1}$) and to the nearest neighbor correlator Φ_{NN} (triangles, see text). The circles in (b) (right-hand scale) display the reduced averaged energy per atom.

with the full solutions of (2) fixes g_m above 700 K with a precision of about 10^{-3}.

The Φ_m parameters are q dependent and are related to the plateau value of Φ_q in the β regime where $g(\Phi)$ takes on its maximum. The deduced g_m values agree for both q sets. For $T \geq 1200$ K the values $g_m < 1$ reflect that the system is clearly in the liquid state. Below 1000 K the system seems near the arrested state. Therefore diffusive currents have to be considered, which according to the extended version of the MCT [6–8] enter the theory by modifying

$$M_0(z) = LT\{h(\tau) + \omega^2 f(\tau)\}_z\,, \tag{7}$$

the Laplace transform of the total damping, into

$$M(z) := [D(z) + M_0(z)^{-1}]^{-1}, \tag{8}$$

where $D(z)$ describes the coupling to the transverse currents. With this substitution Eq. (2) holds, too, but now an apparent $f(\tau)_{\mathrm{app}}$ acts, which follows from the inverse Laplace transformation

$$h(\tau) + \omega^2 f(\tau)_{\mathrm{app}} := LT^{-1}\{M(z)\}_\tau\,. \tag{9}$$

It is a particular result of the present analysis that $f(\tau)_{\mathrm{app}}$ can be mimicked by Eq. (3) with suitable parameters g_m, Φ_m for reproducing $\Phi(\tau)$ by solutions of Eq. (2) in the considered time and temperature window. According to our analysis the system at 1000 K and below is close to the strictly arrested state, but it seems hindered to cross the border. This is the behavior predicted by the MCT when taking into account diffusionlike current fluctuations [6–8]. At the moment we cannot say whether the fluctuations that suppress the strictly arrested state come from insufficient structural relaxations in our MD processing or whether they reflect the inherent thermal motions. Linear extrapolation of the g_m data indicates that the crossover takes place around $T^* \approx 1120$ K, which may be identified with T_c.

The intimate interrelationship between the g_m parameters found here for the two sets of correlation functions is not expected to hold for different correlators. Regarding this we have additionally analyzed the four-point correlator $\Phi_{\mathrm{NN}}(\tau)$, which describes the averaged probability that atom pairs (i, j) forming nearest neighbors at time t are nearest neighbors at time $t + \tau$, too. (Nearest neighbors here are defined by interatomic distances shorter than the minimum between first and second neighbor shells in the partial radial distribution function.) The analysis of the $\Phi_{\mathrm{NN}}(\tau)$ in terms of the schematic MCT equation provides g_m values as indicated by triangles in Fig. 3(b). They differ from those of the Φ_q correlators but yield the same crossover temperature T_c. (Details of the Φ_{NN} correlators and their analysis shall be skipped here for brevity.)

For comparison we have estimated the caloric T_G of the simulated system. Figure 3(b) includes with right-hand scale the reduced energy per atom $\langle E_T \rangle - 3kT$ obtained from averaging over the time evolution of the relaxed system beyond the 10^6 integration steps (corresponding to 2.5 ns) isothermal equilibration of the quenched configurations as described at the beginning. The extrapolated kink in the slope of this plot predicts $T_G \approx 1050$ K, i.e., a MD simulated T_G 70 K below T_c. This result agrees with the finding by Lewis and Wahnström [14] who obtained in the MD modeling of ortho-terphenyl a T_G value (comparable to the experimental one) 30 K below T_c when equilibrating well the undercooled liquid in a way similar to ours. The difference between the estimated T_G and T_c found here is somewhat larger than the commonly accepted value of 30 to 50 K (e.g., [13–15]) between these quantities for molecular glasses. This, however, seems plausible because of the larger T_c in our metallic glass system.

To summarize, the present analysis makes it tempting to use $g_m(T)$ as a relative measure (the value depending on the correlator under consideration) to judge how close the undercooled liquid has approached the idealized structural arrest. With decreasing temperature, $g_m(T)$ approaches the critical value of 1 for structural arrest without, however, exceeding it. Although the $\Phi_q(\tau)$ curves in Figs. 1(a) and 1(b) at first glance show no break in their temperature dependence, g_m from the present analysis clearly reflects the ergodic behavior above T_c (with $g_m < 1$) and the balancing of the system near the border between ergodic and nonergodic behavior below T_c, with crossover in a rather narrow temperature interval. Local relaxations and diffusionlike current fluctuations in the arrested state require that the real system must be characterized through $g_m < 1$ when analyzed in terms of the schematic MCT equation. With $g_m \rightarrow 1$ a drastic increase in the α relaxation time takes place. Therefore, when cooling the system near T_c within a finite rate all the features come together which characterize the glass formation scenario. The system will be found in quenched-in nonequilibrium configurations which undergo irreversible relaxation processes that enter the apparent g_m.

[1] J. Jäckle, Rep. Prog. Phys. **49**, 171 (1986).
[2] W. Götze and L. Sjögren, Rep. Prog. Phys. **55**, 241 (1992).
[3] K. Kawasaki, Physica (Amsterdam) **208A**, 35 (1994).
[4] W. Götze and R. Haussmann, Z. Phys. B **72**, 403 (1988).
[5] W. Götze and L. Sjögren, J. Phys. C **1**, 4203 (1989).
[6] W. Götze and L. Sjögren, J. Phys. C **21**, 3407 (1988).
[7] P. S. Das and G. F. Mazenko, Phys. Rev. A **34**, 2265 (1986).
[8] L. Sjögren, Z. Phys. B **79**, 5 (1990).
[9] F. Mezei, W. Knaak, and B. Fargo, Phys. Rev. Lett. **58**, 571 (1987).
[10] W. van Megen and S. M. Underwood, Phys. Rev. E **49**, 4206 (1994).
[11] E. Rössler, A. P. Sokolov, A. Kisliuk, and D. Quitmann, Phys. Rev. B **49**, 14 967 (1994).
[12] L. J. Lewis, Mater. Sci. Eng. A **133**, 423 (1991).
[13] G. Wahnström, Phys. Rev. A **44**, 3752 (1991).
[14] L. J. Lewis and G. Wahnström, Phys. Rev. E **50**, 3865 (1994).
[15] W. Kob and H. C. Andersen, Phys. Rev. Lett. **73**, 1376 (1994).
[16] W. Kob and H. C. Andersen, Phys. Rev. E **51**, 4626 (1995).
[17] H. Teichler, Phys. Status Solidi B **172**, 325 (1992).
[18] Ch. Hausleitner and J. Hafner, Phys. Rev. B **45**, 115 (1992); **45**, 128 (1992).